Am. J. Hum. Genet. 69:673–684, 2001

Mutations in a Novel Gene with Transmembrane Domains Underlie Usher Syndrome Type 3

Tarja Joensuu,[1,2,3,*] Riikka Hämäläinen,[1,2,*] Bo Yuan,[5] Cheryl Johnson,[5] Saara Tegelberg,[1,2] Paolo Gasparini,[6,7] Leopoldo Zelante,[6] Ulla Pirvola,[4] Leenamaija Pakarinen,[8] Anna-Elina Lehesjoki,[1,2] Albert de la Chapelle,[1,5] and Eeva-Marja Sankila[1,2,3]

[1]The Folkhälsan Institute of Genetics and [2]Department of Medical Genetics, Biomedicum Helsinki, University of Helsinki, [3]Helsinki University Eye Hospital, and [4]Institute of Biotechnology, Helsinki; [5]Human Cancer Genetics Program, The Ohio State University, Columbus; [6]Medical Genetics Service, IRCCS-CSS Hospital, San Giovanni Rotondo, Italy; [7]Telethon Institute of Genetics and Medicine, Naples; and [8]Department of Phoniatrics, University Hospital of Tampere, Tampere, Finland

Usher syndrome type 3 (USH3) is an autosomal recessive disorder characterized by progressive hearing loss, severe retinal degeneration, and variably present vestibular dysfunction, assigned to 3q21-q25. Here, we report on the positional cloning of the *USH3* gene. By haplotype and linkage-disequilibrium analyses in Finnish carriers of a putative founder mutation, the critical region was narrowed to 250 kb, of which we sequenced, assembled, and annotated 207 kb. Two novel genes—*NOPAR* and *UCRP*—and one previously identified gene—H963—were excluded as *USH3,* on the basis of mutational analysis. *USH3,* the candidate gene that we identified, encodes a 120-amino-acid protein. Fifty-two Finnish patients were homozygous for a termination mutation, Y100X; patients in two Finnish families were compound heterozygous for Y100X and for a missense mutation, M44K, whereas patients in an Italian family were homozygous for a 3-bp deletion leading to an amino acid deletion and substitution. *USH3* has two predicted transmembrane domains, and it shows no homology to known genes. As revealed by northern blotting and reverse-transcriptase PCR, it is expressed in many tissues, including the retina.

Introduction

The Usher syndromes (USHs) are characterized by variable degrees of loss of hearing and of loss of eyesight. Three distinct phenotypes have been described. Patients with USH1 have congenital severe-to-profound hearing loss and absence of vestibular function, whereas patients with USH2 have congenital moderate-to-severe hearing loss and normal vestibular function. The onset of retinitis pigmentosa (RP) is prepubertal in patients with USH1 and occurs during the 2d decade of life in patients with USH2 (Smith et al. 1994). Patients with USH3 have postlingual, progressive hearing loss, and the onset of retinitis pigmentosa (RP) symptoms—nyctalopia, progressive constriction of visual fields, and reduction of central visual acuity—usually occurs by the 2d decade of life (Pakarinen et al. 1996). At least 10 loci account for subtypes of USH (see the Hereditary Hearing Loss Homepage). Five genes have so far been identified: *myosin VIIA* (*MYO7A*), for USH1B (MIM 276903) (Weil et al. 1995); *usherin,* for USH2A (MIM 276901) (Eudy et al. 1998); *harmonin,* for USH1C (MIM 276904) (Bitner-Glindzicz et al. 2000; Verpy et al. 2000); *cadherin 23* (*CDH23*), for USH1D (MIM 601067) (Bolz et al. 2001; Bork et al. 2001); and *protocadherin 15* (*PCDH15*), for USH1F (MIM 602083) (Ahmed et al. 2001).

We previously assigned USH3 to 3q21-q25 (Sankila et al. 1995). Significant linkage disequilibrium between USH3 and the linked markers suggested enrichment of a founder mutation in Finland and allowed us to refine the localization of USH3 to a 250-kb genomic interval between markers 107G19CA7 and *D3S3625* (Joensuu et al. 1996, 2000). Haplotype analysis indicated 107G19CA7 to be the proximal historic recombination breakpoint, and a recombination in one family with USH3 placed the *USH3* gene proximal to *D3S3625*. In this study, we (*a*) sequenced, assembled, and annotated 207 kb of the *USH3* critical region, (*b*) excluded two novel genes—*NOPAR* and *UCRP*—and one previously identified gene—H963—as candidates for USH3, and, finally, (*c*) positionally cloned *USH3*.

Subjects and Methods

Families with USH3 and Controls

Clinical and genealogical data on the Finnish and Italian families with USH3 that are studied here also have

Received July 12, 2001; accepted for publication July 31, 2001; electronically published August 27, 2001.

Address for correspondence and reprints: Dr. Eeva-Marja Sankila, The Folkhälsan Institute of Genetics, Biomedicum Helsinki, 00014-University of Helsinki, Finland. E-mail: eeva-marja.sankila@helsinki.fi

* The first two authors contributed equally to this article.

0002-9297/2001/6904-0002$02.00

been described elsewhere (Pakarinen et al. 1995; Sankila et al. 1995; Joensuu et al. 1996, 2000; Gasparini et al. 1998). Control DNA samples from 100 anonymous blood donors from eastern Finland (where there is a high prevalence of USH3) and from 100 donors from western and southern Finland (where there is a low prevalence of USH3) were provided by the Finnish Red Cross Blood Transfusion Service. A total of 51 grandparents in families from the Centre d'Étude du Polymorphisme Humain (CEPH) were also studied as controls.

Bacterial Artificial Chromosome (BAC) DNA and Shotgun Sequencing

We shotgun sequenced partly overlapping BACs—specifically, 355L4 and 545J16. Shotgun libraries were prepared and plasmid DNA was extracted by GATC Shotgun Library Construction service. DNA fragments were ligated to the PCR-Blunt II-Topo cloning vector (Invitrogen), and we sequenced the subclones, from both directions, with custom vector primers designed by GATC and with BigDye-terminator chemistry (PE Applied Biosystems), by use of a PE9700 Thermal Cycler (Perkin Elmer). Sequence readings were transferred to a UNIX-based system; edited and filtered by removal of matches to the cloning and sequencing vectors, as well as to *Escherichia coli,* by the GASP software package (University of Washington Genome Center); and assembled by Phil Green's Phred, Phrap, and Consed sequence-assembly programs. The orientation of contigs, from centromere to telomere, was determined on the basis of the marker order of the physical map described elsewhere (Joensuu et al. 2000).

Computational Analyses and Sequence Annotation by Integrated Gene-Prediction Programs

The complete genomic sequence assembled was masked for repetitive elements, by the RepeatMasker2 program (University of Washington Genome Center). Sequence-similarity searches were performed using BLAST programs (Altschul et al. 1997) against different databases, Human Index for Nonredundant Transcripts (HINT) (Zhuo et al. 2001), UNIGENE (Boguski and Schuler 1995), and the TIGR Human Gene Index (Liang et al. 2000). The sequences were compared with the High-Throughput Genome Sequence and Genomic Survey Sequence databases (National Center for Biotechnology Information), to identify BAC clones or P1-derived artificial clones mapping to the same region. To compare orthologous mouse genomic sequences, homology searches were performed by use of the Celera Assembled and Annotated Mouse Genome. Complete sequence annotation was performed by a modified computational sequence annotation tool, Genotator (Harris 1997), and by the NIX program (UK Human Genome Mapping Project Resource Centre). Transcription-factor and promoter predictions at the 5′-flanking genomic sequences of identified genes were performed by MatInspector/TRANSFAC and Neural Network Promoter Input programs (Baylor College of Medicine Search Launcher). Protein predictions were performed by the PIX program (UK Human Genome Mapping Project Resource Centre), LASERGENE (DNASTAR), TMpred (Swiss Institute of Bioinformatics), SignalP (Center for Biological Sequence Analysis), and PSORT II (Human Genome Center).

DNA and cDNA

We extracted BAC DNA as described elsewhere (Joensuu et al. 2000). Integrated Molecular Analysis of Genomes and Their Expression (IMAGE) cDNA clones for expressed-sequence tags (ESTs) homologous to the *USH3* region were obtained from Research Genetics. To obtain the complete sequence of the inserts, cDNA clones were sequenced on both strands by vector-specific primers.

Human-placenta RNA and Marathon Ready Human Retina cDNA were obtained from Clontech. The first-strand cDNA synthesis was performed with 1 μg of total RNA, according to the supplied protocol for the SMART PCR cDNA Synthesis kit (Clontech). Subsequently, 2 μl of the 100-μl reaction mixture was PCR amplified by gene-specific primers. To isolate full-length cDNAs of the predicted genes, we performed rapid amplification of cDNA ends (RACE) PCR with the Marathon Ready Human Retina cDNA libraries, according to the manufacturer's instructions, by a modified PCR with annealing at 65°C for 1 min 30 s, for 20 cycles, followed by nested PCR with annealing at 60°C for 1 min 30 s, for 40 cycles, in a total volume of 50 μl.

We designed combinations of forward and reverse first-amplification primers and nested primers with the program Primer3 (Whitehead Institute for Biomedical Research/Massachusetts Institute of Technology Center for Genome Research). When possible, the primer pairs were designed to span introns in order to minimize false-positive results by contaminating DNA in the reverse-transcriptase PCRs (RT-PCRs). PCR primer sequences and conditions are available on request.

PCR and RT-PCR

We analyzed candidate genes by PCR amplification and direct sequencing of all exon regions with adjacent splice sites, from genomic DNA and, when possible, from total RNA and poly(A) RNA—using the Qiagen Total RNA kit and the poly(A) RNA–extraction kit provided by Amersham, respectively—from Epstein-Barr virus–transformed lymphoblasts extracted from two patients with USH3, two carriers, and two controls.

Amplification of genomic DNA was performed as described elsewhere (Joensuu et al. 1996). For RT-PCR, either 200 ng of lymphoblast poly(A) RNA or 1 μg of total RNA was primed by random hexamers and was reverse transcribed for the first-strand synthesis of cDNA. Subsequent nested PCR from cDNA was essentially performed with 2 μl of the 20-μl cDNA reaction mix in a total volume of 25 μl with 0.2 mM of each dNTP, 20 pmol of each primer, and 0.5 U of Ampli*Taq* Gold DNA polymerase (PE Applied Biosystems). Control reactions containing human genomic DNA and water, without cDNA, were performed. Amplification of GC-rich regions was attempted with 1.2 mM betaine or 7% dimethyl sulfoxide.

We electrophoresed PCR products on either 1%–2% SeaKem agarose gel or 0.7 × MDE SSCP (FMC) polyacrylamide gels and visualized them by ethidium-bromide or silver staining (Bassam et al. 1991). Direct sequencing of the purified amplification products (PCR purification kit; Qiagen) was performed by automated sequencing (ABI 377-sequencer; PE Applied Biosystems) by use of the PCR primers.

Analysis of Novel Single-Nucleotide Polymorphisms (SNPs)

By genomic sequencing of *NOPAR*, in families with USH3, we identified novel SNPs—RSNP2 and TSNP1, in *NOPAR* introns 1 and 9, respectively. Intronic forward and reverse primers used in the genotyping of the families with USH3 were as follows: TSNP1 (forward, 5′-TGGTAGGTAATCTTAGTCCAACAA-3′; reverse, 5′-TTTTGCCTCACATAGAATGGTG-3′), 390 bp; and RSNP2 (forward, 5′-CATGCACCAAGCTCTCACAT-3′; reverse, 5′-AAGCTGAGGGAAGAAACTGC-3′), 264 bp. The alleles were detected either by direct sequencing or by SSCP analysis, in 0.7 × MDE gel, for 18 h at 5 W, at room temperature. The SSCP alleles were visualized by silver staining. Haplotypes were manually constructed under the assumption that there were a minimum number of recombinations.

Isolation of the Candidate Gene USH3

The interexon 5′- and 3′-UTR primers used in combining the exons from cDNA synthesized, by PCR (conditions were as described above), from human-retina total RNA or the Marathon Ready Human Retina cDNA library (Clontech) were as follows: E3F (5′-CTCCTGTGGCTGTCTTGTCA-3′) and W27577R (5′-TGGTGGGTTTGCCTCTTAGT-3′); E2F (5′-AAGCAATCCCAGTGAGCATC-3′) and E3R (5′-TGACAAGACAGCCACAGGAG-3′); E1F (5′-TCACTATCTGAAACTATCTTGTTGT-3′) and E2R (5′-TAGGGGACCATGCAGAGTTT-3′); and E1F2 (5′-TGCCTCCCCACCATTCACCA–3′) and E2R2 (5′-CATGAAGAAGGCTGTCCCCACCA-3′).

Mutation Detection

Using genomic DNA, we amplified genomic fragments encompassing five *USH3* exons, by use of the following intronic primers: E1F (see above) and P1R (5′-AAGCCCCTGAACTTTATAGG-3′), 910 bp; P1BF (5′-TTGTGGCCATTTTTGGAGAT-3′) and P1BR (5′-CCCCAAACATGTATCAAGTGC-3′), 207 bp; P2F (5′-TCAGAAGGATTTTAGTGATGTTTGA-3′) and P2R (5′-TCTTTTTGACATATTGAAAAGCACA-3′), 352 bp; P3F (5′-ATGTCAATGGGGATGATGGT-3′) and P3R (5′-GGAGCCCATTCAGAAAATGA-3′), 291 bp; and P4F (5′-TTCCCCTGAATTACCCATCA-3′) and P4R (5′-AGCATCTGGAAACTCGGTGT-3′), 339 bp. PCR products were purified and sequenced as described above.

The Fin_{major} mutation and the Italian 3-bp deletion were screened by direct sequencing of the 291-bp product amplified by primers P3F and P3R. For the Fin_{minor} mutation, we used SSCP; a 198-bp fragment was PCR amplified by primers P2F2 (5′-TCCCAGTGAGCATCCACGTC-3′) and P2R2 (5′-TGAAAAGCACATTTGTCTTCAGAGG-3′), and the alleles were separated on 0.7 × MDE gels, for 18 h at 5 W, at room temperature and were visualized by silver staining.

Northern Blot and In Situ Hybridization

A human multiple-tissue northern blot from 12 adult tissues was hybridized by use of an $\alpha[^{32}P]$-dCTP random-labeled cDNA probe (*USH3* nucleotides −33–321; 354 bp) comprising exons 1–3 and part of the 5′ UTR. The membrane was washed at 65°C with 2 × SSC (saline sodium citrate) and 0.05% SDS, then exposed to x-ray film at −80°C for 2 d. In situ hybridization and the production of cRNA probes were performed as described by Wilkinson and Green (1990). In short, 4% paraformaldehyde–fixed paraffin sections from embryonic 16-d-old mouse embryos and from dissected adult eyes and inner ears were used for analysis. A 262-bp fragment from the Marathon Ready Mouse Brain cDNA library (Clontech) was produced by primers mouse/p1 (5′-ATCCCCGTAAGCATCCACAT-3′) and mouse/p2 (5′-TTCTGTAGGCATAGGTCCCTTC-3′). The amplified fragment was cloned into the pGEM-T Easy vector (Promega) according to the manufacturer's instructions. Subsequently, $[^{35}S]$-labeled antisense and control-sense cRNA probes were synthesized by in vitro transcription. The control-sense probe did not produce any hybridization signal above background level.

Results

Construction of the Genomic Contigs and Transcript Map

We chose two partly overlapping BAC clones (355L4 and 545J16) flanking both 107G19CA7 and most of the

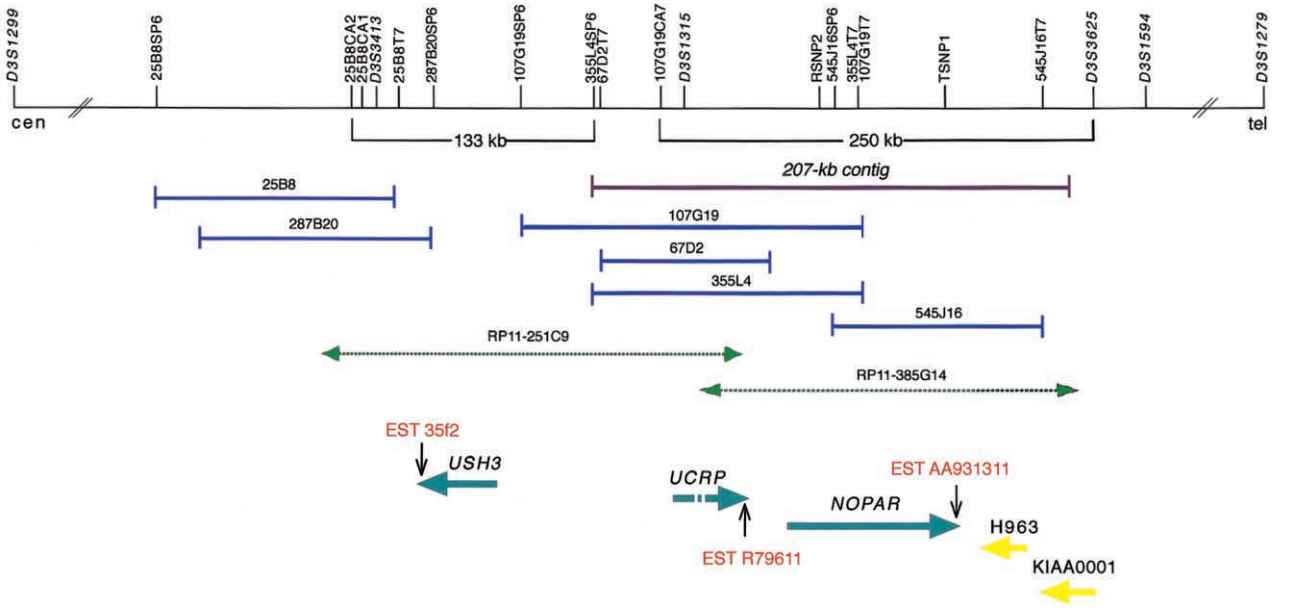

Figure 1 Schematic representation of physical and transcript maps covering the *USH3* region, depicting the initial 250-kb *USH3* region and the extended 133-kb *USH3* region, with partly overlapping BAC clones. Polymorphic markers and sequence-tagged sites are indicated by vertical lines. Previously mapped BAC clones are shown in dark blue, and the 207-kb sequence contig assembled is indicated by a purple line. Database-derived and partly assembled BAC sequences from clones RP11-385G14 and RP11-251C9 are indicated by green dashed arrows. The centromere is on the left. A pair of previously known genes—KIAA0001 and H963—and a group of three novel genes—*NOPAR, UCRP,* and *USH3*—are indicated by yellow and light-blue arrows, respectively, showing the orientation of transcription. ESTs representing parts of the 3′ UTRs of the transcripts are indicated by vertical arrows. H963, *NOPAR, UCRP,* and *USH3* were subjected to mutation analyses in this study.

previously defined *USH3* critical region toward *D3S3625,* for shotgun sequencing. Database-derived BAC clone RP11-385G14 sequence was aligned with genomic contigs of BAC clone 545J16, to extend the distal sequences. Gap filling was performed by primer walking from the contig end sequences and by PCR across the gaps. A final sequence contig of 207 kb, which is depicted in figure 1, was assembled.

Use of nucleotide-nucleotide BLAST for searches of the contig identified 30 distinct or partly overlapping human ESTs and 11 orthologous mouse or rat ESTs (table 1). Starting from the identified ESTs and exons predicted by GRAIL and GENESCAN, we used a combination of RT-PCR, RACE experiments, and direct PCR of cDNA libraries, to assemble two novel genes: *NOPAR* (for no opposite-paired repeat) and *UCRP* (for USH critical region pseudogene) (fig. 1). We identified two alternatively spliced transcripts—*NOPAR* and *NOPAR2*—which encode putative polypeptide isoforms, of 721 and 756 amino acids, respectively, showing 61% identity to the amino terminus of *TRAP230* (Ito et al. 1999), also called the "human OPA-containing gene," or "*HOPA*" (Philibert et al. 1999). The *NOPAR* coding region comprises approximately one-third of the length of *TRAP230/HOPA* and lacks the 3′ OPA repeat contained in *TRAP230/HOPA*. Northern blot analysis of *NOPAR* showed widespread expression in adult tissues (data not shown). Transcription in human retina was shown by RT-PCR.

The 2,045 bp of *UCRP* cDNA obtained consists of five exons spanning >70 kb genomic DNA. However, the open reading frame (ORF) is disrupted, and the gene thus is probably an unprocessed pseudogene. The region also contained two previously identified genes: KIAA0001 (Nomura et al. 1994), which was previously excluded as *USH3* (Joensuu et al. 2000), and platelet-activating–receptor homolog mRNA H963 (Jacobs et al. 1997).

Refinement of the USH3 *Critical Region*

The exons and flanking intronic sequences of *NOPAR, UCRP,* and H963 were examined for mutations in patients with USH3; however, no potential disease-causing mutations were detected. Genomic sequencing of the *NOPAR* introns in patients with USH3 indicated the presence of two novel SNPs, RSNP2 (nucleotide C/G) and TSNP1 (nucleotide T/C), in introns 1 and 9, respectively (fig. 1). Haplotype analysis revealed conservation of the segment RSNP2–TSNP1 in all 48 *USH3* chromosomes studied (data not shown). This supported our previous haplotype analysis placing *USH3* distal to 107G19CA7 (Joensuu et

Table 1

Location of ESTs in the 207-kb Contig

EST	Location(s)	GenBank Accession Number	dbEST Details
1	24264–24640	R75628	*Homo sapiens* cDNA clone IMAGE: 143509 3′
2	65074–65380	R79610	*H. sapiens* cDNA clone IMAGE: 146349 5′
3	65715–65825	T39157	*H. sapiens* cDNA clone IMAGE: 60197 5′
4	66204–66483	T40442	*H. sapiens* cDNA clone IMAGE: 60197 3′
5	66139–66502	R79611	*H. sapiens* cDNA clone IMAGE: 146349 3′
6	78227–78422, 107727–107829, 114184–114230	AI501968	*Rattus norvegicus* cDNA clone UI-R-C0-jb-b-08-0-UI 3′
7	78227–78422, 107727–107829, 114184–114251	AW920576	EST351880 Bento Soares *R. norvegicus* cDNA clone RGIGZ01 5′
8	79115–79401	AW897677	CM1-NN0062-280400-202-d05 NN0062 *H. sapiens* cDNA
9	79118–79401	AW897669	CM1-NN0062-280400-202-b05 NN0062 *H. sapiens* cDNA
10	99994–100283	AA776659	*H. sapiens* cDNA clone IMAGE: 970436 3′
11	78227–78422, 107727–107829, 114184–114241	BE948099	UI-M-BH3-aws-h-03-0-UI.s1 *Mus musculus* cDNA clone UI-M-BH3-aws-h-03-0-UI 3′
12	136681–136758	AF062710	AF062710 *H. sapiens* cDNA clone HA0028
13	136681–136758	AI110602	*H. sapiens* cDNA HA0028
14	181289–181421	AA931311	*H. sapiens* cDNA clone IMAGE: 1565326 3′
15	186110–186218	BE843843	RC0-TN0079-310700-021-b10 TN0079 *H. sapiens* cDNA
16	186131–186641	AA170490	*M. musculus* cDNA clone IMAGE: 618166 5′
17	186185–186518	AW591154	*H. sapiens* cDNA clone IMAGE: 2703652 3′
18	186193–186446	BB209769	BB209769 *M. musculus* cDNA clone A430094C06 3′
19	186193–186773	BE283279	601101050F1 *M. musculus* cDNA clone IMAGE: 3493212 5′
20	186235–186446	AI172577	*R. norvegicus* cDNA clone UI-R-C2p-nz-h-03-0-UI 3′
21	186313–186789	AA162789	*M. musculus* cDNA clone IMAGE: 598871 5′
22	186665–187193, 190857–190910	AV653286	AV653286 GLC *H. sapiens* cDNA clone GLCDJC11 3′
23	186660–187193, 190857–190910	AV653266	AV653266 GLC *H. sapiens* cDNA clone GLCDJB03 3′
24	186676–187016	AV757663	*H. sapiens* cDNA clone: BMFBHF02, 5′ end
25	186903–187075	AA184698	*M. musculus* cDNA clone IMAGE: 634121 3′
26	186952–187148	AI592667	*M. musculus* cDNA clone IMAGE: 634121 5′
27	187086–187195, 190857– 190954	AA353758	EST61951 *H. sapiens* cDNA 5′
28	200484– 201179	AU138895	*H. sapiens* cDNA clone: PLACE1009521, 5′
29	204146– 204843	AL042755	*H. sapiens* mRNA; EST DKFZp434C0522_r1
30	199885– 200422	AU157802	*H. sapiens* cDNA clone: PLACE1009521, 3′
31	205968– 206348	AL042756	*H. sapiens* mRNA; EST DKFZp434C0522_s1
32	199885–200231	AI167543	Soares_NhHMPu_S1 *H. sapiens* cDNA clone IMAGE: 1661439 3′
33	199883–200242	AA027011	Soares_pregnant_uterus_NbHPU *H. sapiens* cDNA clone IMAGE: 469358 3′
34	199885–200183	AI277229	Soares_placenta_8to9weeks_2NbHP8to9W *H. sapiens* cDNA clone IMAGE: 1893709 3′
35	206135–206348	AI889440	*H. sapiens* cDNA clone IMAGE: 2444461 3′
36	200575–200753	AA026830	*H. sapiens* cDNA clone IMAGE: 469358 5′
37	200005–200189	AI686699	*H. sapiens* cDNA clone IMAGE: 2268648 3′
38	200580–200783	R35752	Soares placenta Nb2HP *H. sapiens* cDNA clone IMAGE: 136983 5′
39	202796–202998	AA056078	Soares retina N2b4HR *H. sapiens* cDNA clone IMAGE: 381530 3′
40	201215–201642	AI050350	*M. musculus* cDNA clone IMAGE: 1379171 5′
41	199880–200139	R35645	*H. sapiens* cDNA clone IMAGE: 136983 3′

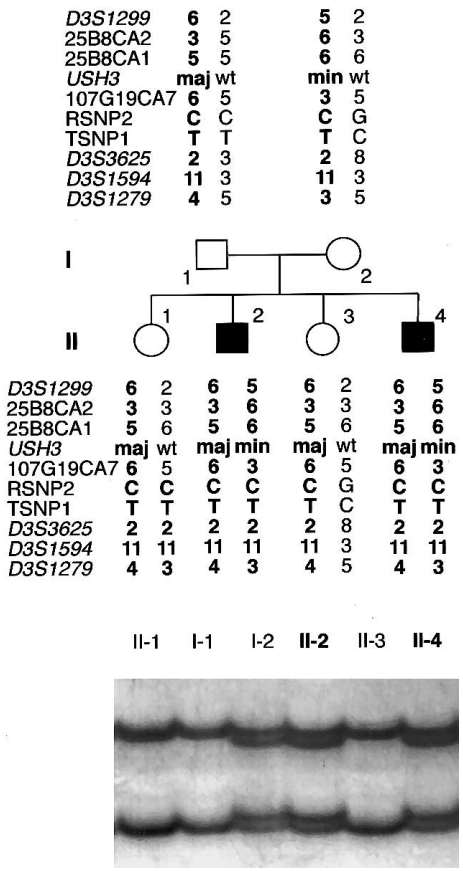

Figure 2 Pedigree of a Finnish family with USH3, segregating a paternal Fin_{major} mutation (maj)—c.300T→G—and a maternal Fin_{minor} mutation (min)—c.131T→A. Alleles at seven microsatellite markers, two SNPs, and *USH3* are shown; wt = wild type. The chromosomes assumed to carry the disease allele are in boldface type. The father carries a conserved ancestral haplotype, whereas the mother's disease-associated haplotype shares alleles at the RSNP2–*D3S1594* segment only. A recombination in the maternal chromosome of individual II-1 excludes the segment RSNP2–*D3S1279* as the site of the *USH3* mutation. At the bottom is the result of an SSCP analysis used in the detection of the Fin_{minor} mutation. A mobility shift caused by the mutation was detected in individuals I-2, II-2, and II-4.

al. 2000); however, a recombination event in one family excluded the RSNP2-TSNP1-tel segment as the site of the causative mutation (fig. 2). No additional transcripts in the remaining 60-kb critical region between markers 107G19CA7 and RSNP2 were found. This implicated the region immediately centromeric to 107G19CA7 and extending to 25B8CA2, as part of the *USH3* critical region.

Identification of the USH3 *Gene*

We assembled database-derived RP11-251C9 sequences between 107G19CA7 and 25B8CA2. BLAST analyses of the newly constructed 133-kb contig revealed 11 ESTs (data not shown). Starting from a retina-derived EST 35f2 and exons predicted in its vicinity, a contiguous cDNA sequence of 1,444 bp was obtained by RT-PCR of human retina-derived total RNA (a gift from F. P. M. Cremers) and by PCR of Marathon Ready Human Retina cDNA. Sequence analysis suggested a 360-bp ORF comprising four exons that span ~18 kb at the genomic level. By comparison of the genomic sequence with the *USH3* cDNA sequence, the exon-intron boundaries and their flanking sequences were confirmed and were in agreement with the consensus GT-AG splicing rule. A splice variant, *USH3* isoform b, comprising an additional 87-bp exon (1b) with an in-frame stop codon between exons 1 and 2 was also detected. The first in-frame ATG codon in exon 1 conforms with the Kozak motif (Kozak 1987). No splice acceptor was found at the 5′ end of exon 1, suggesting that this exon is the first. There is a 5′ UTR of ⩾392 bp and a 3′ UTR of ⩾692 bp. Computational promoter analysis revealed five possible promoters for *USH3*. The putative promoter regions lack TATA boxes but include CAAT and GC boxes. Three alternative polyadenylation signals were found, at 156 bp, 764 bp, and 3,568 bp downstream of the termination codon, consistent with both the northern blot analysis showing three transcripts, of 4.5 kb, 1.5 kb, and 1.0 kb, respectively, and expression in many adult-human tissues (fig. 3). Expression was also detected in adult-human retina, by RT-PCR. Only human lymphoblasts did not show a signal, as confirmed by both RT-PCR and northern blotting.

The analysis with the Celera Assembled and Annotated Mouse Genome indicated several genomic fragments highly homologous to exons 2 and 3 of *USH3*. In situ hybridization with [^{35}S]-labeled riboprobes corresponding to the orthologous mouse sequence showed a low-level, ubiquitous expression in several mouse tissues (data not shown).

The candidate gene *USH3* encodes a novel, putative transmembrane protein of 120 amino acids with a calculated molecular mass of 13.4 kD (fig. 4). It shows no homology to previously known genes or proteins. Bioinformatics analyses suggest a cytosolic amino terminus, two helical transmembrane domains (residues 25–41 and 63–79), and a putative endoplasmic-reticulum membrane–retention signal, TKGH, in the carboxy terminus.

USH3 *Mutations*

We identified three causative mutations in Finnish and Italian patients with USH3 (fig. 5). The Finnish founder mutation is a nonsense mutation, c.300T→G in exon 3 (Y100X, or Fin_{major}), predicting the truncation of 21 amino acids. Fin_{major} was found in 52 patients with USH3 who were homozygous for a conserved ancestral haplotype, whereas all 36 parents analyzed and 26 of 45 unaffected siblings were heterozygous for the mutation. The second Finnish mutation is a c.131T→A transversion at codon 44 in exon 2, resulting in an amino acid

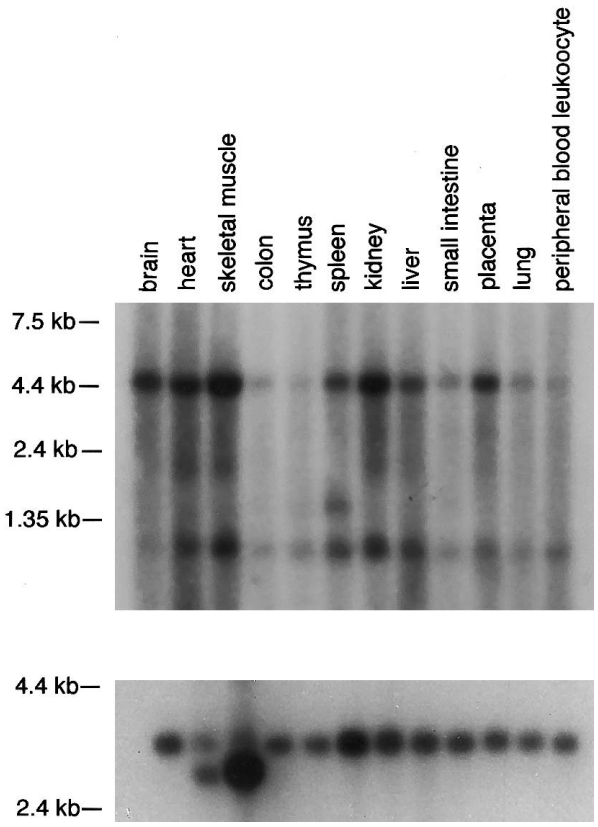

Figure 3 *USH3* expression. Northern analysis of an adult-human multiple-tissue blot was performed by use of a probe comprising the coding region of *USH3*. Two signals, of ~4.5 kb and ~1.0 kb, are detected in all tissues. In addition, a weak signal, of ~1.5 kb, is detected in spleen mRNA. The blot was hybridized with a β-actin probe as a control (*bottom*).

substitution of lysine for methionine (M44K, or Fin_{minor}). In two Finnish families, four patients are compound heterozygous for Fin_{major} and Fin_{minor}. These patients have inherited the common ancestral haplotype, from one parent, and a partly distinctive haplotype, from the other parent (fig. 2). The Fin_{minor} mutation originates from the same region in eastern Finland where USH3 is known to be prevalent. In a consanguineous Italian family with USH3 showing linkage to the 3q21-q25 markers (Gasparini et al. 1998), we detected a homozygous 3-bp deletion, c.231–233delATT in exon 3, resulting in the substitution of one methionine for isoleucine and leucine at codons 77 and 78.

By direct sequencing (in the case of Fin_{major} and the Italian mutation, c.231–233delATT) and by SSCP analysis (in the case of Fin_{minor}), none of either 100 anonymous blood donors from southern and western Finland or 51 grandparents in families from the CEPH were found to carry any of the three mutant alleles. Of 100 anonymous blood donors from eastern Finland, 1 was heterozygous for Fin_{major}. This was expected, because USH3 is clustered in eastern Finland (Pakarinen et al. 1995).

Discussion

The association of RP with sensorineural deafness is named "USH." More than 60 genes responsible for RP and for related disorders have been identified (Retnet), and, to date, ~20 genes for nonsyndromic deafness are known. Products of RP genes include phototransduction proteins, photoreceptor structural proteins, transcription factors, and proteins involved in metabolism of the photoreceptor and of the retinal pigment epithelium. The recent identification of several deafness genes by molecular genetic studies has enabled the investigation of the molecular basis of normal and pathological auditory function. The genes encode proteins that have a role in hair-cell transduction, in ionic homeostasis in the cochlear duct, and in integrity of the tectorial membrane (Steel and Kros 2001).

Five genes underlying USH have been identified in previous studies. Mutations of *myosin VIIA* cause nonsyndromic deafness as well as USH1B (Weil et al. 1995; Liu et al. 1997*a*, 1997*b*). The *shaker-1* mice with *myo7a* mutations show progressive disorganization of the stereocilia bundle (Self et al. 1998). Although there is no retinal degeneration in *shaker-1* mice, abnormal accumulation of opsin in the connecting cilium of photoreceptors and a failure of melanosome transport in the retinal pigment epithelium have been detected (Liu et al. 1998, 1999; Liu and Williams 2001). It is thought that harmonin interacts with myosin VIIA in the sensory cells of the inner ear, and *harmonin* mutations underlie USH1C as well as autosomal recessive nonsyndromic deafness DFNB18 (Verpy et al. 2000). Surprisingly, no *harmonin* expression was detected in neonatal-mouse eyes (Verpy et al. 2000), whereas anti-harmonin staining was found in portions of the developing-human eyes (Bitner-Glindzicz et al. 2000). Mutations in two novel cadherin-related genes—*CDH23* and *PCDH15*—are responsible for USH1D and USH1F, respectively (Ahmed et al. 2001; Bolz et al. 2001; Bork et al. 2001). Disorganized stereocilia in the corresponding deaf-mouse mutants *waltzer* (Di Palma et al. 2001) and *Ames waltzer* (Alagramam et al. 2001) indicate that cadherins are involved in either the lateral links or the tip links that join adjacent stereocilia, although no gross retinal pathology has been detected in these mouse models. Humans with *CDH23* mutations show variable retinal symptoms or, as in autosomal recessive nonsyndromic deafness DFNB12, no retinal phenotype at all (Bolz et al. 2001; Bork et al. 2001). USH2A, as well as nonsyndromic RP, is caused by mutations in *usherin,* which

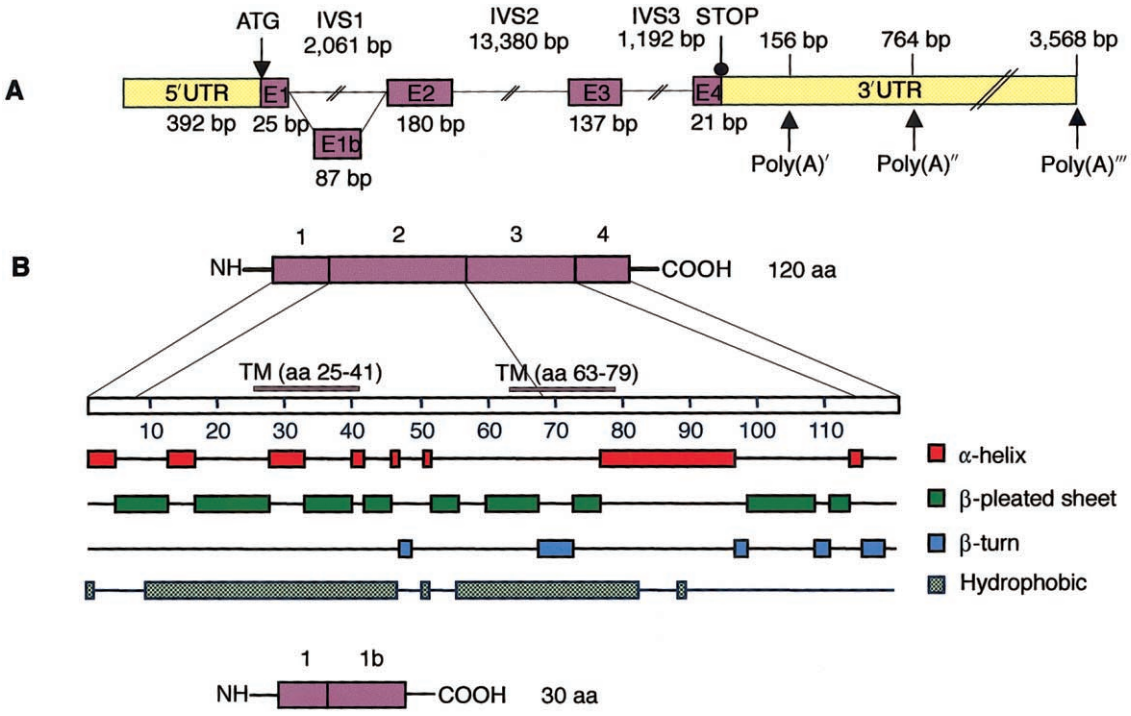

Figure 4 Predicted schematic structure and regions of secondary structure in the human *USH3* gene and in USH3 protein. *A,* The five exons of *USH3,* depicted by numbered boxes (E1–E4). The lengths of the exons are shown below the boxes, and those of the three separating introns are shown above the lines. The translation-initiation site and the first stop codon are indicated. Three polyadenylation signals (Poly(A)) and their predicted locations downstream of the termination codon are indicated by arrows. *B,* One-hundred-twenty-amino-acid protein, encoded by *USH3,* with two predicted transmembrane domains, at residues 25–41 and 63–79. The combination of putative secondary structures, such as α-helices, β-pleated sheets, and β-turns, features possible functional protein domains. An alternatively spliced transcript (*bottom*) of *USH3* predicts a 30-amino-acid protein.

encodes a putative extracellular-matrix protein (Eudy et al. 1998; Rivolta et al. 2000).

Our results demonstrate that a gene encoding a 120-amino-acid protein with two predicted transmembrane domains and no homology to previously known proteins underlies USH3. In contrast to previously characterized USH genes that show distinct expression patterns in the sensory structures of the inner ear and of the retina, *USH3* shows ubiquitous expression in several tissues. However, two genes involved in nonsyndromic X-linked RP—*RP2* and *RPGR*—are also ubiquitously expressed but, nonetheless, have an important and specific role in the retina (Roepman et al. 1996; Schwahn et al. 1998). Patients with USH3 are born with normal hearing and vision, and the progressive sensory defects start later in life, leading to profound hearing loss, variable vestibular dysfunction, and severe RP with nyctalopia, constriction of the visual fields, and loss of central visual acuity.

Previously, we assigned, by linkage, a *USH3* locus to 3q21-q25 and established the existence of a USH subtype characterized by postlingual, progressive hearing loss (Sankila et al. 1995). That cases of USH3 comprise ~40% of all cases of USH in Finland has been explained by a founder effect. Families with USH showing linkage to the *USH3* region have also been reported in the United States and Sweden (Kimberling et al. 1995), Spain (Espinos et al. 1998), Israel (Adato et al. 1999), and Italy (Gasparini et al. 1998). Using the significant linkage disequilibrium observed in the Finnish families with USH3, we were able to refine the *USH3* critical region to 250 kb (Joensuu et al. 2000). The entire segment was subcloned, sequenced, and assembled, resulting in a 207-kb–sequence contig with 30 human ESTs. Three genes (*NOPAR, UCRP,* and H963)—two of which were novel—were identified and excluded as candidates, by sequencing. Of these, *UCRP* is probably an unprocessed pseudogene; however, interestingly, *NOPAR* shows significant homology to a thyroid-hormone receptor–associated protein, TRAP230 (Ito et al. 1999). The candidate gene that we identified, *USH3,* lies outside the initial critical region defined by haplotype analyses. This is explained by the fact that two mutations instead of the expected one founder mutation were found to segregate in the Finnish families with USH3. The Finnish founder mutation, c.300T→G in

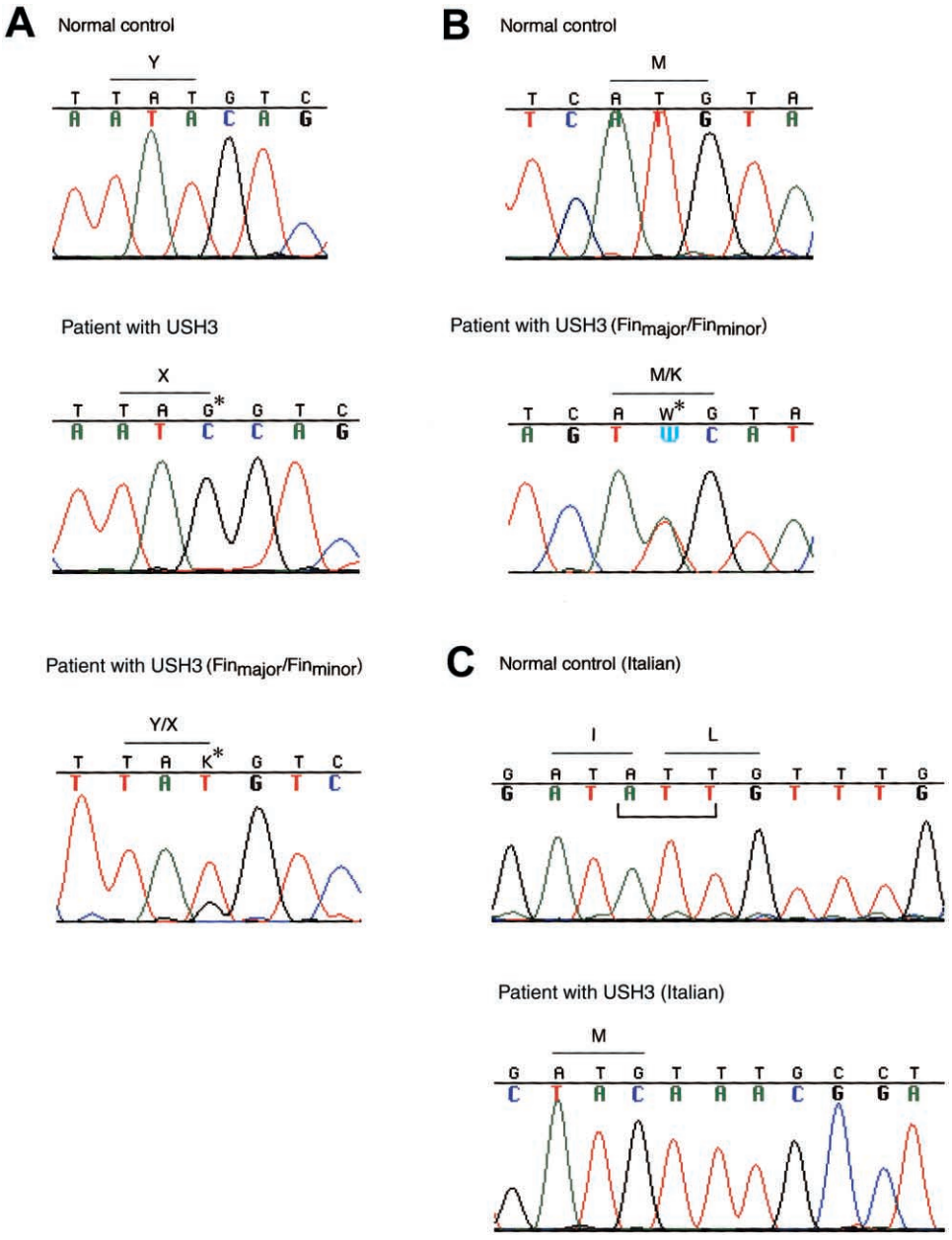

Figure 5 Detection of three different mutations segregating in families with USH3. *A*, Sequence analysis of a genomic PCR fragment comprising exon 3 in a normal control, in a patient with USH3 who is homozygous for the ancestral Fin_{major} mutation—c.300T→G (resulting in Y100X)—in a heterozygous carrier, and in a compound heterozygous patient (Fin_{major}/Fin_{minor}). Positions of mutated nucleotides are indicated by arrows and asterisks. *B*, Finnish mutation Fin_{minor}—c.131T→A (resulting in M44K) in exon 2: sequence chromatograms of a control and of a compound-heterozygous patient with USH3 (Fin_{major}/Fin_{minor}). *C*, Sequence chromatograms of a control, of a homozygous patient, and of a heterozygous carrier, representing the Italian mutation—a 3-bp deletion, c.231–233delATT—in exon 3. The deletion results in the substitution of one methionine for isoleucine and leucine. The deleted nucleotides are indicated below the normal control sequence.

exon 3, was found in all *USH3* chromosomes with the Finnish ancestral haplotype. It leads to a premature stop codon, which most probably affects mRNA stability or produces a truncated protein. In two Finnish families, patients were heterozygous for Fin_{major} and a c.131T→A transversion resulting in an amino acid substitution of lysine for methionine. In an Italian family with USH3, a homozygous 3-bp deletion, c.231–233delATT in exon 3, was detected. Among 200 Finnish controls and 51 individuals from the CEPH families, 1 Finnish individual was, as expected, heterozygous for the Fin_{major} mutation, whereas neither of the other two mutations was

detected. Although the biochemical mechanisms by which *USH3* causes retinal and cochlear disease remain to be elucidated, the identification of *USH3* will already enable exact and even presymptomatic diagnosis of the disease.

Acknowledgments

We thank the patients and their families for cooperation, Ms. Sinikka Lindh for collecting the Finnish USH3 samples, Dr. Pertti Sistonen for providing the Finnish control samples, Dr. Angelo Notarangelo for preparing the Italian USH3 cell lines, Drs. Robert Chadwick and Lars Paulin for sequencing assistance, and Dr. Jose Dieguez for technical and computational advice and helpful discussions. This study was supported by the Ulla Hjelt Fund, the Finnish Eye and Tissue Bank Foundation, the Finnish Eye Foundation, Finnish State grants TYH8222 and TYH9235, the Academy of Finland, National Institutes of Health grant CA16058, and Telethon grant E.813.

Electronic-Database Information

Accession numbers and URLs for data in this article are as follows:

Baylor College of Medicine Search Launcher, http://searchlauncher.bcm.tmc.edu/ (for MatInspector/TRANSFAC and Neural Network Promoter Input programs)

BLAST, http://www.ncbi.nlm.nih.gov/BLAST/

Celera Publication Site, http://publication.celera.com/ (for Assembled and Annotated Mouse Genome)

Expressed Sequence Tags Database, http://www.ncbi.nlm.nih.gov/dbEST/

GenBank, http://www.ncbi.nlm.nih.gov/Genbank/ (for 207-kb contig sequence [accession number AF388363], BAC clones RP11-385G14 [accession number AC011103] and RP11-251C9 [accession number AC020636], human *NOPAR* coding sequence [accession number AF388364], human *NOPAR2* coding sequence [accession number AF388365], human *UCRP* putative pseudogene sequence [accession number AF388367], human *HOPA* coding sequence [accession number AF132033], human H963 coding sequence [accession number AF002986], human *TRAP230* mRNA [accession number NM_005120], human KIAA0001 coding sequence [accession number NM_014879], EST 35f2 sequence [accession number W27577], and cDNA of *USH3* [accession number AF388366] and of a splice variant, *USH3* isoform b [accession number AF388368], of *USH3*)

Genome Survey Sequences Database, http://www.ncbi.nlm.nih.gov/dbGSS/

Hereditary Hearing Loss Homepage, http://www.uia.ac.be/dnalab/hhh/ (for loci accounting for subtypes of USH)

High-Throughput Genomic Sequences, http://www.ncbi.nlm.nih.gov/HTGS/

Human Cancer Genetics BioInformatics at the Ohio State University, http://pandora.med.ohio-state.edu/HINT/ (for HINT database)

Online Mendelian Inheritance in Man (OMIM), http://www.ncbi.nlm.nih.gov/Omim/ (for USH1B [MIM 276903], USH1C [MIM 276904], USH1D [MIM 601067], USH1F [MIM 602083], and USH2A [MIM 276901])

Phred/Phrap/Consed System Home Page, The, http://www.phrap.org/ (for Phred, Phrap, and Consed sequence-assembly programs)

Primer3 Software Distribution, http://www-genome.wi.mit.edu/genome_software/other/primer3.html

PSORT WWW Server, http://psort.nibb.ac.jp/ (for PSORT II)

RepeatMasker Web Server, http://ftp.genome.washington.edu/cgi-bin/RepeatMasker (for RepeatMasker2)

RetNet: Retinal Information Network, http://www.sph.uth.tmc.edu/Retnet/ (for genes responsible for RP and related disorders)

SignalP V1.1 World Wide Web Prediction Server, http://www.cbs.dtu.dk/services/SignalP/

TIGR Human Gene Index, http://www.tigr.org/tdb/hgi/

TMpred: Prediction of Transmembrane Regions and Orientation, http://www.ch.embnet.org/software/TMPRED_form.html

UK Human Genome Mapping Project Resource Centre, http://www.hgmp.mrc.ac.uk/ (for NIX and PIX program packages)

University of Washington Genome Center, http://www.genome.washington.edu/UWGC/ (for GASP software package)

References

Adato A, Kalinski H, Weil D, Chaib H, Korostishevsky M, Bonne-Tamir B (1999) Possible interaction between USH1B and USH3 gene products as implied by apparent digenic deafness inheritance. Am J Hum Genet 65:261–265

Ahmed ZM, Riazuddin S, Bernstein SL, Ahmed Z, Khan S, Griffith AJ, Morell RJ, Friedman TB, Riazuddin S, Wilcox ER (2001) Mutations of the protocadherin gene *PCDH15* cause Usher syndrome type 1F. Am J Hum Genet 69:25–34

Alagramam KN, Murcia CL, Kwon HY, Pawlowski KS, Wright CG, Woychik RP (2001) The mouse Ames Waltzer hearing-loss mutant is caused by mutation of *Pcdh15,* a novel protocadherin gene. Nat Genet 27:99–102

Altschul SF, Madden TL, Schäffer AA, Zhang J, Zhang Z, Miller W, Lipman DJ (1997) Gapped BLAST and PSI-BLAST: a new generation of protein database search programs. Nucleic Acids Res 25:3389–3402

Bassam BJ, Caetano-Anolles G, Gresshoff PM (1991) Fast and sensitive silver staining of DNA in polyacrylamide gels. Anal Biochem 196:80–83

Bitner-Glindzicz M, Lindley KJ, Rutland P, Blaydon D, Smith VV, Milla PJ, Hussain K, Furth-Lavi J, Cosgrove KE, Shepherd RM, Barnes PD, O'Brien RE, Farndon PA, Sowden J, Liu XZ, Scanlan MJ, Malcolm S, Dunne MJ, Aynsley-Green A, Glaser B (2000) A recessive contiguous gene deletion causing infantile hyperinsulinism, enteropathy and deafness identifies the Usher type 1C gene. Nat Genet 26:56–60

Boguski MS, Schuler GD (1995) ESTablishing a human transcript map. Nat Genet 10:369–371

Bolz H, von Brederlow B, Ramirez A, Bryda EC, Kutsche K, Nothwang HG, Seeliger M, del C-Salcedó Cabrera M, Vila MC, Molina OP, Gal A, Kubisch C (2001) Mutation of *CDH23,* encoding a new member of the cadherin gene family, causes Usher syndrome type 1D. Nat Genet 27:108–112

Bork JM, Peters LM, Riazuddin S, Bernstein SL, Ahmed ZM, Ness SL, Polomeno R, et al (2001) Usher syndrome 1D and nonsyndromic autosomal recessive deafness DFNB12 are caused by allelic mutations of the novel cadherin-like gene *CDH23*. Am J Hum Genet 68:26–37

Di Palma F, Holme RH, Bryda EC, Belyantseva IA, Pellegrino R, Kachar B, Steel KP, Noben-Trauth K (2001) Mutations in *Cdh23*, encoding a new type of cadherin, cause stereocilia disorganization in waltzer, the mouse model for Usher syndrome type 1D. Nat Genet 27:103–107

Espinos C, Najera C, Millan JM, Ayuso C, Baiget M, Perez-Garrigues H, Rodrigo O, Vilela C, Beneyto M (1998) Linkage analysis in Usher syndrome type I (USH1) families from Spain. J Med Genet 35:391–398

Eudy JD, Weston MD, Yao SF, Hoover DM, Rehm HL, Ma-Edmonds M, Yan D, Ahmad I, Cheng JJ, Ayoso C, Cremers C, Davenport S, Moller C, Talmadge CB, Beisel KW, Tamayo M, Morton CC, Swaroop A, Kimberling WJ, Sumegi J (1998) Mutation of a gene encoding a protein with extracellular matrix motifs in Usher syndrome type IIa. Science 280:1753–1757

Gasparini P, De Fazio A, Croce AI, Stanziale P, Zelante L (1998) Usher syndrome type III (USH3) linked to chromosome 3q in an Italian family. J Med Genet 35:666–667

Harris NL (1997) Genotator: a workbench for sequence annotation. Genome Res 7:754–762

Ito M, Yuan CX, Malik S, Gu W, Fondell JD, Yamamura S, Fu ZY, Zhang X, Qin J, Roeder RG (1999) Identity between TRAP and SMCC complexes indicates novel pathways for the function of nuclear receptors and diverse mammalian activators. Mol Cell 3:361–370

Jacobs KA, Collins-Racie LA, Colbert M, Duckett M, Golden-Fleet M, Kelleher K, Kriz R, LaVallie ER, Merberg D, Spaulding V, Stover J, Williamson MJ, McCoy JM (1997) A genetic selection for isolating cDNAs encoding secreted proteins. Gene 198:289–296

Joensuu T, Blanco G, Pakarinen L, Sistonen P, Kääriäinen H, Brown S, Chapelle A, Sankila EM (1996) Refined mapping of the Usher syndrome type III locus on chromosome 3, exclusion of candidate genes, and identification of the putative mouse homologous region. Genomics 38:255–263

Joensuu T, Hämäläinen R, Lehesjoki A-E, de la Chapelle A, Sankila E-M (2000) A sequence-ready map of the Usher syndrome type III critical region on chromosome 3q. Genomics 63:409–416

Kimberling WJ, Weston MD, Moller C, van Aarem A, Cremers CW, Sumegi J, Ing PS, Connolly C, Martini A, Milani M, Tamayo ML, Bernal J, Greenberg J, Ayuso C (1995) Gene mapping of Usher syndrome type IIa: localization of the gene to a 2.1-cM segment on chromosome 1q41. Am J Hum Genet 56:216–223

Kozak M (1987) An analysis of 5′-noncoding sequences from 699 vertebrate messenger RNAs. Nucleic Acids Res 15: 8125–8148

Liang F, Holt I, Pertea G, Karamycheva S, Salzberg SL, Quackenbush J (2000) Gene index analysis of the human genome estimates approximately 120,000 genes. Nat Genet 25:239–240

Liu X, Ondek B, Williams DS (1998) Mutant myosin VIIa causes defective melanosome distribution in the RPE of shaker-1 mice. Nat Genet 19:117–118

Liu X, Udovichenko IP, Brown SD, Steel KP, Williams DS (1999) Myosin VIIA participates in opsin transport through the photoreceptor cilium. J Neurosci 19:6267–6274

Liu XZ, Walsh J, Mburu P, Kendric-Jones J, Cope MJ, Steel KP, Brown SD (1997*a*) Mutations in the myosin VIIA gene cause non-syndromic recessive deafness. Nat Genet 16:188–190

Liu XZ, Walsh J, Tamagawa Y, Kitamura K, Nishizawa M, Steel KP, Brown SD (1997*b*) Autosomal dominant non-syndromic deafness caused by a mutation in the myosin VIIA gene. Nat Genet 17:268–269

Liu X, Williams DS (2001) Coincident onset of expression of myosin VIIa and opsin in the cilium of the developing photoreceptor cell. Exp Eye Res 72:351–355

Nomura N, Miyajima N, Sazuka T, Tanaka A, Kawarabayasi Y, Sato S, Nagase T, Seki N, Ishikawa K, Tabata S (1994) Prediction of the coding sequences of unidentified human genes. I. The coding sequences of 40 new genes (KIAA0001–KIAA0040) deduced by analysis of randomly sampled cDNA clones from human immature myeloid cell line KG-1. DNA Res 1:47–56

Pakarinen L, Sankila E-M, Tuppurainen K, Karjalainen S, Kääriäinen H (1995) Usher syndrome type III (USH3): the clinical manifestations in 42 patients. Scand J Logoped Phoniatr 20:141–150

Pakarinen L, Tuppurainen K, Laippala P, Mäntyjärvi M, Puhakka H (1996) The ophthalmological course of Usher syndrome type III. Intl Ophthalmol 19:307–311

Philibert RA, Winfield SL, Damschroder-Williams P, Tengstrom C, Martin BM, Ginns EI (1999) The genomic structure and developmental expression patterns of the human OPA-containing gene (*HOPA*). Hum Genet 105:174–178

Rivolta C, Sweklo EA, Berson EL, Dryja TP (2000) Missense mutation in the *USH2A* gene: association with recessive retinitis pigmentosa without hearing loss. Am J Hum Genet 66:1975–1978

Roepman R, van Duijnhoven G, Rosenberg T, Pinckers AJ, Bleeker-Wagemakers LM, Bergen AA, Post J, Beck A, Reinhardt R, Ropers HH, Cremers FP, Berger W (1996) Positional cloning of the gene for X-linked retinitis pigmentosa 3: homology with the guanine-nucleotide-exchange factor RCC1. Hum Mol Genet 5:1035–1041

Sankila EM, Pakarinen L, Kääriäinen H, Aittomäki K, Karjalainen S, Sistonen P, de la Chapelle A (1995) Assignment of an Usher syndrome type III (USH3) gene to chromosome 3q. Hum Mol Genet 4:93–98

Schwahn U, Lenzner S, Dong J, Feil S, Hinzmann B, van Duijnhoven G, Kirschner R, Hemberger M, Bergen AA, Rosenberg T, Pinckers AJ, Fundele R, Rosenthal A, Cremers FP, Ropers HH, Berger W (1998) Positional cloning of the gene for X-linked retinitis pigmentosa 2. Nat Genet 19:327–332

Self T, Mahony M, Fleming J, Walsh J, Brown SD, Steel KP (1998) Shaker-1 mutations reveal roles for myosin VIIA in both development and function of cochlear hair cells. Development 125:557–566

Smith RJ, Berlin CI, Hejtmancik JK, Keats BJ, Kimberling WJ, Lewis RA, Moller CG, Pelias MZ, Tranebjaerg L, Usher

Syndrome Consortium (1994) Clinical diagnosis of the Usher syndromes. Am J Med Genet 50:32–38

Steel KP, Kros CJ (2001) A genetic approach to understanding auditory function. Nat Genet 27:143–149

Verpy E, Leibovici M, Zwaenepoel I, Liu XZ, Gal A, Salem N, Mansour A, Blanchard S, Kobayashi I, Keats BJ, Slim R, Petit C (2000) A defect in harmonin, a PDZ domain-containing protein expressed in the inner ear sensory hair cells, underlies Usher syndrome type 1C. Nat Genet 26:51–55

Weil D, Blanchard S, Kaplan J, Guilford P, Gibson F, Walsh J, Mburu P, Varela A, Levilliers J, Weston MD, Kelley PM, Kimberling WJ, Wagenaar M, Levi-Acobas F, Larget-Piet D, Munnich A, Steel KP, Brown SDM, Petit C (1995) Defective myosin VIIA gene responsible for Usher syndrome type 1B. Nature 374:60–61

Wilkinson DG, Green DK (1990) *In situ* hybridization and three-dimensional reconstruction of serial sections. In: Copp AJ, Cockroft DL (eds) Postimplantation mammalian embryos: a practical approach. IRL press, Oxford, pp 151–171

Zhuo D, Zhao WD, Wright FA, Yang H-Y, Wang J-P, Sears R, Baer T, Kwon D-H, Gordon D, Gibbs S, Dai D, Yang Q, Spitzner J, Krahe R, Stredney D, Stutz A, Yuan B (2001) Assembly, annotation, and integration of UNIGENE clusters into the Human Genome Draft. Genome Res 11:904–918